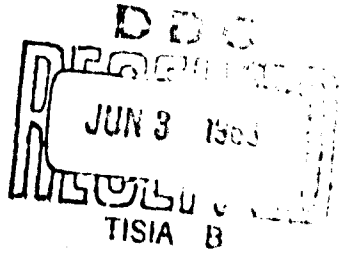

HYDRONAUTICS, incorporated
research in hydrodynamics

Research, consulting, and advanced engineering in the fields of NAVAL and INDUSTRIAL HYDRODYNAMICS. Offices and Laboratory in the Washington, D. C., area: Pindell School Road, Howard County, Laurel, Md.

TECHNICAL REPORT 119-4

ON FINITE LENGTH CAVITIES BENEATH A FREE SURFACE

by

B. Yim

December 1962

Prepared under

Bureau of Ships
Department of the Navy
Contract No. NObs-84296

ABSTRACT

The two-dimensional flow under a free surface with non-zero cavitation number is considered using a "point drag" cavity model. The drag coefficient is obtained in closed form as a function of the cavitation number and the curvature at the cavity end (or nose), but not explicitly of the depth. The thickness-length-ratio of the cavity is calculated numerically and compared with the case of an elliptic cylinder under a free surface.

The three dimensional effect on the cavity is also considered by the approximation of the cavity to an ellipsoid.

These results should be of use in the estimation of the shape of cavities behind ventilated hydrofoil wings and in the subsequent calculation of downwash.

TABLE OF CONTENTS

LIST OF SYMBOLS

A	constant defined in Equation [4]
a, b	constants in the transformed plane given in Equation [2] and Figure 2
Ar	area given in Section 10
C	curvature
C_D =	$D/\frac{1}{2}\rho U_o^2$
C_p	pressure coefficient
D	drag
d	depth of foil
E.F.	first and second kinds of incomplete elliptic integrals respectively
K, $\bar{E}$, Π	first, second, and third kinds of complete elliptic integrals respectively
H_o	homogeneous solution defined in Section 4
Im =	imaginary part of
k, k'	constants associated with elliptic integrals defined in Section 10
ℓ	length of cavity
L	scale factor of transformation
P$\int$	principal value of integral
q(x)	source distribution as function of x
s	semi-span
t	maximum thickness of cavity

U_o	velocity at ∞
U_{max}	maximum velocity on the body
$w=u-iv$	complex velocity nondimensionalized with respect to U_o
u_H, v_H	real variables defined in Equation [4]
$v_x(a,b,c)$	x component of the incremental velocity at (a,b,c)
ρ	density
σ	cavitation number
$\zeta=\xi+\eta i$	transformed plane

LIST OF FIGURES

HYDRONAUTICS, Incorporated

ON FINITE LENGTH CAVITIES BENEATH A FREE SURFACE

1. INTRODUCTION

Fully cavitated hydrofoils under a free surface at infinite Froude number and non-zero cavitation number in two dimensional flow are considered. Using a method previously used by Fabula (1960) and Wu (1957) we compute the point drag acting on the end of the linearized hydrofoil-cavity system. Thus we obtain the relations between drag, length, and thickness of the cavity for a given depth of foil and cavitation number.

Rapid progress in the development of high speed hydrofoil boats has led to a need for an understanding of cavity flows beneath a free surface. Although the case of zero cavitation number has been developed a great deal in recent years [e.g., Jakob Auslaender (1961), V. E. Johnson (1958)], the mathematical difficulty in dealing with a doubly connected domain has retarded the investigation of the case of finite length cavities (non-zero cavitation number) under a free surface.

Wu (1957) pointed out that the calculation of the drag from the flow field near the trailing cavity end singularity in the linear theory has the same physical basis as the calculation of drag on the image body in the Riabouchinsky model or the determination of the jet momentum in the reentrant jet model. Fabula (July, 1960) used a two dimensional, linearized model of a cavity in an infinite fluid symmetric with respect to the vertical axis. This model, which may be considered as a linearized Riabouchinsky model, is called "a point drag cavity model", and has the same singularities at the leading and the rear edge respectively. Fabula (July, 1960) calculated the point drag, and cavity length-thickness-ratio, and obtained surprisingly good agreement with the nonlinear

Riabouchinsky model [Plesset, M. S., and Shaffer, P. A., Jr. (1948), and Byrne Perry (1952)]. He also considered the effect of the presence of two symmetrically located solid boundaries parallel to the flow direction with this model (October 1960).

This report is an extension of the method used by Fabula to the calculation of the point drag and the cavity size in the presence of a free surface.

2. FORMULATION OF PROBLEM

Figure 1a shows the cavity and the coordinate system used in this report. Since in the linearized theory perturbations are taken as very small, the cavity shown in Figure 1a may be assumed to represent the boundary of the thin slit shown in Figure 1b. The line $y = d$ represents the free surface and the slit at $y = 0$, and $0 < x \leq \ell$, the cavity in the z plane. u is the x component, and v is the y component of the perturbation velocity nondimensionalized with respect to the free stream velocity U_o. The boundary conditions for the analytic complex velocity w are as follows. Froude number is assumed to be very large so that it can be approximated to ∞. Accordingly, u is equal to zero on the free surface $y = d$. On the cavity $u = \frac{\sigma}{2}$, where σ is the cavitation number [see Tulin (1953)]. Since the flow is considered to be exactly symmetric with respect to the $x = \frac{\ell}{2}$ axis, u is symmetric and v is anti-symmetric with respect to $X = x - \frac{\ell}{2}$. Hence

$$u(X) = u(-X),$$

and

$$v(X) = - v(-X).$$

It then follows that

$$v(0) = 0$$

on the axis $X = 0$, or $x = \frac{\ell}{2}$. In view of these considerations it is necessary to consider only one half of the physical plane (Figure 1c). The boundary conditions for the complex velocity $w(z) = u - iv$ in this plane may be summarized as follows:

On the free surface	$E_\infty D$	$u = 0$	
On the center line	DC, AE_∞	$v = 0$	
On the cavity	BC, BA	$u = \sigma/2$	
At $\lvert z \rvert = \infty$		$w(z) = 0$	[1]
On $z = 0$, $w(z)$ behaves like $\frac{1}{\sqrt{z}}$ (R. T. Jones, 1960)			
On pt. D		$w(z) = 0$	

There is no singularity except at $z = 0$ in the half plane.

3. TRANSFORMATION OF THE PHYSICAL PLANE

We now transform the forward half of the z plane under the free surface $y = d$ into the upper half of the ζ plane (Figure 1d) by means of the Schwarz-Christofell transformation

$$\frac{dZ}{d\zeta} = \frac{L\,(\zeta - b)}{(\zeta^2 - 1)^{\frac{1}{2}}\,(\zeta - a)^{\frac{1}{2}}} \qquad [2]$$

where constants L, a, and b will be determined later. The boundary conditions given by Equation [1] become in the upper half of the $\zeta(=\xi + i\eta)$ plane as follows:

$$
\left.
\begin{array}{ll}
\text{On } -1 < \xi < 1 & u = \sigma/2 \\
\left.\begin{array}{l} -\infty < \xi < -1 \\ 1 < \xi < a \end{array}\right\} & v = 0 \\
a < \xi < \infty & u = 0 \\
\xi = a & w(\zeta) = 0 \\
\text{As } |\zeta| \to \infty & w(\zeta) \to 0
\end{array}
\right\} \quad [3]
$$

At $\zeta = b$ $w(\zeta)$ behaves like $\dfrac{1}{\zeta - b}$

and there is no other singularity except at $\zeta = b$ on the upper half of the ζ plane.

Notice u and v are alternately prescribed on the real axis.

4. SOLUTION

It is now necessary to find an analytic function $w(\zeta)$ on the upper half of the ζ plane satisfying boundary conditions of Equations [3] on the real axis of ζ plane. Cheng and Rott (1954) have developed a general method for solving such boundary value problems when u and v are given alternately on the real axis. The first step is to find the homogeneous solution $H_o(\zeta)$. This solution satisfies the boundary conditions of Equation [3] with the following exceptions: at $-1 < \xi < 1$ the condition $u = \sigma/2$ is changed to $u = 0$, and the boundary conditions at ∞ may be violated.

Under these conditions

$$H_o(\zeta) = \frac{iA(\zeta^2 - 1)^{\frac{1}{2}} (\zeta - a)^{\frac{1}{2}}}{\zeta - b} \equiv u_H - i\, v_H \qquad [4]$$

where A is constant. According to Cheng and Rott the uniqueness of the solution satisfying boundary conditions [3] is assured, in this case, by $H_o(\zeta) \not\to 0$ as $|\zeta| \to \infty$, but

$$\frac{H_o(\zeta)}{\xi - \zeta} \to 0 \quad \text{as} \quad |\zeta| \to \infty .$$

We notice here from [4]

$$v_H(\xi, 0) = - \frac{A(\xi^2 - 1)^{\frac{1}{2}} (\xi - a)^{\frac{1}{2}}}{\xi - b}$$

$$\text{on} \; -1 < \xi < 1 .$$

We now find a new function $\frac{w(\zeta)}{H_o(\zeta)}$ which is also analytic in the upper half of the ζ plane except at certain points on the real axis. The usefulness of this function is that when combined with boundary conditions [3] and Equation [4] its imaginary part is determined on the whole real axis.

$$\frac{w(\zeta)}{H_o(\zeta)} = \frac{u - iv}{u_H - iv_H} \qquad [5]$$

According to the definition of $H_o(\zeta)$, $u_H = 0$ on the portions where $u(\xi, 0)$ is prescribed. Thus, equating the imaginary part of Equation [5], we have

$$\mathrm{Im}\left(\frac{w(\xi,0)}{H_o(\xi,0)}\right) = \frac{u(\xi,0)}{v_H(\xi,0)} = \frac{-(\xi-b)\frac{\sigma}{2}}{A(\xi^2-1)^{\frac{1}{2}}(\xi-a)^{\frac{1}{2}}} \qquad [6]$$

$$\text{on } |\xi| < 1$$

$$= 0 \qquad \text{on } \xi > a$$

Similarly on the portion where $v(\xi,0)$ is prescribed,

$$v_H(\xi,0) = 0, \quad v(\xi,0) = 0.$$

We then have

$$\mathrm{Im}\left(\frac{w(\xi,0)}{H_o(\xi,0)}\right) = \frac{v(\xi,0)}{u_H(\xi,0)} = 0 \; . \qquad [7]$$

Now using the formula for the analytic function on the half plane with the given imaginary value on the real axis [see e.g. Philip M. Morse, Herman Feshbach, Part I (1953)]

$$\frac{w(\zeta)}{H_o(\zeta)} = \frac{1}{\pi} \int_{-\infty}^{\infty} \frac{\mathrm{Im}\left(\frac{w(\xi,0)}{H_o(\xi,0)}\right)}{\xi - \zeta} \, d\xi \qquad [8]$$

we have, inserting the values [6] and [7] in Equation [8]

$$w(\zeta) = -\frac{\sigma H_o(\zeta)}{2A\pi} \int_{-1}^{1} \frac{(\xi - b)\, d\xi}{(\xi-\zeta)(\xi^2-1)^{\frac{1}{2}}(\xi-a)^{\frac{1}{2}}} \qquad [9]$$

Now substituting the expression of $H_o(\zeta)$ in Equation [4] into above equation and performing the integration we obtain

$$w(\zeta) = u(\zeta) - iv(\zeta) = - \frac{i\sigma(\zeta^2-1)^{\frac{1}{2}}(\zeta-a)^{\frac{1}{2}}}{2\pi(\zeta-b)} \int_{-1}^{1} \frac{(\xi-b)\,d\xi}{(\xi-\zeta)(\xi^2-1)^{\frac{1}{2}}(\xi-a)^{\frac{1}{2}}}$$

$$= - \frac{i\sigma(\zeta^2-1)^{\frac{1}{2}}(\zeta-a)^{\frac{1}{2}}}{2\pi(\zeta-b)} \int_{-1}^{1} \left\{ \frac{1}{(\xi^2-1)^{\frac{1}{2}}(\xi-a)^{\frac{1}{2}}} + \frac{\zeta-b}{(\xi-\zeta)(\xi^2-1)^{\frac{1}{2}}(\xi-a)^{\frac{1}{2}}} \right\} d\xi$$

$$= - \frac{i\sigma(\zeta^2-1)^{\frac{1}{2}}(\zeta-a)^{\frac{1}{2}}}{2\pi(\zeta-b)} \left[\frac{-2}{\sqrt{a+1}} K\left(\sqrt{\frac{2}{a+1}}\right) + (\zeta-b) \int_{-1}^{1} \frac{d\xi}{(\xi-\zeta)(\xi^2-1)^{\frac{1}{2}}(\xi-a)^{\frac{1}{2}}} \right] \qquad [10]$$

where K is the first kind of complete elliptic integral. Near $\zeta = b$ the last integral behaves like $(\zeta-b)\,\Pi$, where the third kind of elliptic integral Π has at most logarithmic singularities.

When we use the Plemelj formula [I. I. Privalov (1919), or Muskhelichvili (1946)]

$$\lim_{\zeta \to t} \int_{-1}^{1} \frac{\phi(\xi)}{\xi-\zeta}\,d\xi = \pi i \phi(t) + P \int_{-1}^{1} \frac{\phi(\xi)}{\xi-t}\,d\xi$$

where t is on the real axis $(-1 < t < 1)$ and P $\int$ is the principal part of the integral, we can easily show that Equation [10] is our solution satisfying all the given conditions.

5. DRAG

Using the formula for the point drag by Wu (1957) or by the Blasius theorem we obtain

$$C_D = \frac{\text{drag}}{\frac{1}{2}\rho U_o^2} = -\,\mathrm{Im} \oint_{z=0} w^2(z)\,dz$$

$$= -\,\mathrm{Im} \int_{\zeta=b} w^2(\zeta)\,\frac{dz}{d\zeta}\,d\zeta$$

$$= \mathrm{Im} \int_{\zeta=b} \frac{L\sigma^2(\zeta^2-1)^{\frac{1}{2}}(\zeta-a)^{\frac{1}{2}}K\left(\sqrt{\frac{2}{a+1}}\right)}{\pi^2\,(\zeta-b)\,(a+1)}\,d\zeta$$

$$+ \text{------}$$

where + ------ indicates the terms which do not contribute to the residue. Now if we take the integral along the small semi-circle at $\zeta = b$ using the value of the residue, we obtain

$$C_D = \frac{\sigma^2 L\sqrt{(1-b^2)(a-b)}}{\pi\,(a+1)}\;K^2\left(\sqrt{\frac{2}{a+1}}\right) \qquad [11]$$

constants a, b, and L are determined from the correspondence between the z and ζ planes. When the depth of the foil becomes infinite, we can show that as $a \to \infty$, L behaves like $\frac{\ell}{2}\sqrt{a}$; as $b \to 0$ $K^2 \to \left(\frac{\pi}{2}\right)^2$, and

$$C_D \to \frac{\pi}{8}\,\ell\sigma^2 \,, \qquad [12]$$

which agrees with Fabula's result for the case of infinite submergence.

This is also shown in Figure 2 where the value of $C_D/\sigma^2 \ell$ at $d/\ell = 1.5$ is already close to $\pi/8$.

6. MAXIMUM CAVITY THICKNESS

The maximum thickness of the cavity is obtained by integrating the y component velocity on the cavity boundary ($0 \leq x \leq \frac{\ell}{2}$, $y = 0$)

$$t = \int_0^{\ell/2} v\left(\xi(x+)\right) dx - \int_0^{\ell/2} v\left(\xi(x-)\right) dx$$

$$= \int_b^1 v(\xi) \frac{dx}{d\xi} \, d\xi - \int_b^{-1} v(\xi) \frac{dx}{d\xi} \, d\xi$$

$$= - P \frac{\sigma L}{2\pi} \int_{-1}^{1} \int_{-1}^{1} \frac{(h-b) \, dh \, d\xi}{(\xi-h)(1-h^2)^{\frac{1}{2}}(a-h)^{\frac{1}{2}}}$$

$$= - \frac{\sigma L}{2\pi} \int_{-1}^{1} \frac{(h-b) \log \left|\frac{1-h}{1+h}\right|}{(1-h^2)^{\frac{1}{2}}(a-h)^{\frac{1}{2}}} \, dh$$

or

$$\frac{t}{\frac{\sigma}{2} L} = \frac{1}{\pi} \int_{-1}^{1} \frac{(h-b) \log \left|\frac{1+h}{1-h}\right|}{(1-h^2)^{\frac{1}{2}}(a-h)^{\frac{1}{2}}} \, dh$$

$$= \lim_{\epsilon \to 0} \frac{1}{\pi} \int_0^{1-\epsilon} \frac{\log \left|\frac{1+h}{1-h}\right|}{(1-h^2)^{\frac{1}{2}}} \left[\frac{h-b}{(a-h)^{\frac{1}{2}}} + \frac{h+b}{(a+h)^{\frac{1}{2}}}\right] dh$$

$$- \frac{1}{\pi\sqrt{2}} \left(\frac{1-b}{(a-1)^{\frac{1}{2}}} + \frac{1+b}{(a+1)^{\frac{1}{2}}}\right) \left[2\sqrt{\epsilon} \log \epsilon - 4\sqrt{\epsilon} - 2 (\log 2)\sqrt{\epsilon}\right]$$

If we put $h = \cos\theta$, $(h^2-1)^{\frac{1}{2}}$ in the denominator will be cancelled and only a logarithmic singularity, which is integrable, remains. This integral has been evaluated numerically on an IBM 1620 for sufficiently small ϵ. The curve of $t/(\ell\sigma)$ versus d/ℓ is shown in Figure 3, where d is given by Equation [16a]. The error is less than

$$\pm\left[2\sqrt{\epsilon}\log\epsilon - 4\sqrt{\epsilon} - 2(\log 2)\sqrt{\epsilon}\right]\left\{\frac{1}{\pi\sqrt{2}}\left(\frac{1-b}{(a-1)^{\frac{1}{2}}} + \frac{1+b}{(a+1)^{\frac{1}{2}}}\right)\right.$$

$$\left. - \frac{1}{\pi\sqrt{2-\epsilon}}\left(\frac{1-\epsilon-b}{(a-1+\epsilon)^{\frac{1}{2}}} + \frac{1-\epsilon+b}{(a+1-\epsilon)^{\frac{1}{2}}}\right)\right\}$$

As far as the approximate value of the maximum thickness is concerned, it may be obtained easily. We know from linearized aerofoil theory that a thin elliptic cylinder in a uniform flow has a uniform pressure on its surface [R. T. Jones (1960)]. Even in the presence of a free surface, when the depth is large the effect of the free surface image above is very small. When the depth is nearly zero, the velocity near the body is nearly uniform since the image source distribution is of same magnitude and opposite sign as that under the free surface. Therefore we can say that the pressure on the surface of the submerged elliptic cylinder near the free surface is still approximately uniform.

From the table given by Jones (1960, p.18) for a thin elliptic cylinder whose major axis is at $-1 \leq x \leq 1$

$$u - iv = \frac{t}{\ell}\left(1 - \frac{z}{\sqrt{z^2-1}}\right)$$

where $z = x + yi$

or

$$\sigma_\infty = 2u = 2\frac{t}{\ell}$$

where σ_∞ denotes the cavitation number in the infinite medium. For the effect of the free surface we have only to consider a biplane image above (at y = d). ($0 \leq x \leq \ell$ the distribution of sources is the same as that of the cavity in magnitude but of opposite sign.) Approximately the value of u at x = 0,

$$\frac{\sigma_d}{2} = u = \frac{t}{\ell} \frac{4\, d/\ell}{\sqrt{1 + \left(\frac{4d}{\ell}\right)^2}}$$

where σ_d is the cavitation number for the depth d. If we approximate the cavity under a free surface by an elliptic cylinder

$$\frac{t}{\sigma_d \ell} = \frac{\sqrt{1 + \left(\frac{4d}{\ell}\right)^2}}{8\, \frac{d}{\ell}} \qquad [14]$$

From this, a curve of $\frac{t}{\sigma_d \ell}$ versus $\frac{d}{\ell}$ is shown in Figure 3 with the case of the point drag model. This indicates that the values of $\frac{t}{\ell}$ almost coincide in both cases except between the values of d/ℓ 0.15 and 0.5 where the point drag model differs by at most 0.15 from the elliptic model.

7. CORRESPONDENCE BETWEEN z AND ζ PLANES

If we integrate Equation [2] from $x = \frac{\ell}{2}$ to any point $0 < x < \frac{\ell}{2}$ for y = 0 we obtain from an integral table [Wolfgang Grӧbner and Nikolaus Hofreiter (1958)]

$$x = \frac{2L}{\sqrt{a+1}} \left\{ (a-b)\, F(\phi,k) - (a+1)\, E(\phi,k) \right\} + \frac{\ell}{2} \qquad [15]$$

where

$0 \leq \phi \leq \frac{\pi}{2}$, $k = \sqrt{\frac{2}{a+1}}$, $\xi = 2 \sin^2 \phi - 1$ and F and E are incomplete elliptic integrals.

We note the correspondence of points between the z and ζ plane

$z = \frac{\ell}{2} \quad \sim \quad \zeta = -1$ and 1

$z = \frac{\ell}{2} + id \quad \sim \quad \zeta = a$

$z = 0 \quad \sim \quad \zeta = b$

Inserting these conditions in Equation [15] we obtain

$$0 = \frac{2L}{\sqrt{a+1}} \left[(a-b)\, K\left(\sqrt{\frac{2}{a+1}}\right) - (a+1)\, \overline{E}\left(\sqrt{\frac{2}{a+1}}\right) \right] \qquad [16a]$$

$$d = \frac{2L}{\sqrt{a+1}} \left[-(1+b)\, K\left(\sqrt{\frac{a-1}{a+1}}\right) + (a+1)\, \overline{E}\left(\sqrt{\frac{a-1}{a+1}}\right) \right] \qquad [16b]$$

$$\ell = -\frac{4L}{\sqrt{a+1}} \left[(a-b)\, F\left(\phi, \sqrt{\frac{2}{a+1}}\right) - (a+1)\, E\left(\phi, \sqrt{\frac{2}{a+1}}\right) \right] \qquad [16c]$$

where

$\phi = \sin^{-1} \sqrt{\frac{b+1}{2}}$

K and $\overline{E}$ are complete elliptic integrals.

We obtain the relation between a and b from Equation [16a]

$$b = a - (a + 1)\ \frac{\bar{E}\left(\sqrt{\frac{2}{a+1}}\right)}{K\left(\sqrt{\frac{2}{a+1}}\right)} \qquad [17a]$$

Combining Equations [16b] and [16c]

$$\frac{d}{\ell} = \frac{\left[-(1+b)\ K\left(\sqrt{\frac{a-1}{a+1}}\right) + (a+1)\ \bar{E}\left(\sqrt{\frac{a-1}{a+1}}\right)\right]}{-2\left[(a-b)\ F\left(\phi, \sqrt{\frac{2}{a+1}}\right) - (a+1)\ E\left(\phi, \sqrt{\frac{2}{a+1}}\right)\right]} \qquad [17b]$$

Dividing Equation [11] by Equation [16c] we obtain

$$\frac{C_D}{\sigma^2} = \frac{\sqrt{(b^2-1)}\ (b-a)\ K^2\left(\sqrt{\frac{2}{a+1}}\right)}{-4\pi\left[(a-b)\ F\left(\phi, \sqrt{\frac{2}{a+1}}\right) - (a+1)\ E\left(\phi, \sqrt{\frac{2}{a+1}}\right)\right]\sqrt{a+1}} \qquad [18]$$

$C_D/\sigma^2\ell$ versus d/ℓ is plotted in Figure 2. It shows that $C_D/\sigma^2\ell$ becomes nearly the same as the value at infinite depth when the depth-length ratio of the cavity (d/ℓ) becomes 1.

8. CURVATURE AT THE END POINTS

The curvature at x = 0 (or ξ = b) is obtained from

$$C = \frac{\frac{d^2y}{dx^2}}{\left\{1 + \left|\frac{dy}{dx}\right|^2\right\}^{3/2}}$$

$$\frac{dy}{dx} = \frac{v\left(\xi(x)\right)}{1 + \sigma/2}$$

Thus

$$C = \lim_{\xi \to b} \frac{-\dfrac{\sigma(\xi^2-1)(\xi-a)}{2\pi L(\xi-b)^3(1+\frac{\sigma}{2})} \displaystyle\int_{-1}^{1} \frac{(t-b)\,dt}{(t-\xi)(t^2-1)^{\frac{1}{2}}(t-a)^{\frac{1}{2}}}}{\left\{1 + \left(\dfrac{(\xi^2-1)^{\frac{1}{2}}(\xi-a)^{\frac{1}{2}}}{(1+\frac{\sigma}{2})\pi(\xi-b)} \displaystyle\int_{-1}^{1} \frac{(t-b)\,\frac{\sigma}{2}\,dt}{(t-\xi)(t^2-1)^{\frac{1}{2}}(t-a)^{\frac{1}{2}}} \right)^2 \right\}^{3/2}}$$

$$C = \frac{\pi^2 (1+\frac{\sigma}{2})^2}{L(1-b^2)^{\frac{1}{2}}(a-b)^{\frac{1}{2}}} \left\{ \frac{\sigma}{\sqrt{a+1}} K\left(-\sqrt{\frac{2}{a+1}}\right) \right\}^{-2} \qquad [19]$$

since $$\int_{-1}^{1} \frac{dt}{(t^2-1)^{\frac{1}{2}}(t-a)^{\frac{1}{2}}} = \frac{-2}{\sqrt{a+1}} K\left(-\sqrt{\frac{2}{a+1}}\right)$$

Combining Equations [19] and [11] we obtain

$$C_D = \frac{\pi (1+\frac{\sigma}{2})^2}{C} \qquad [20]$$

That is, the drag coefficient is proportional to the radius of curvature at the nose, for a given cavitation number. It is interesting to note that this relation is independent of the depth.

9. REMARKS

Since it was not necessary to specify the geometry of the body generating the point drag cavity, there are not enough conditions to obtain the length of the cavity or the drag separately. However, when the drag of the body can be estimated by the case of infinite depth (M. P. Tulin, 1953) or zero cavitation number (V. E. Johnson, 1958, or Jakob Auslaender, 1961) since drag is not sensitive to these parameters, it is possible to determine the cavity length, maximum thickness and hence the flow field about the cavity.

10. THREE DIMENSIONAL EFFECT ON THE CAVITY FLOW

Since a two dimensional cavity can be approximated by the known solution of the flow past an elliptic body, it may be worth while to see the three dimensional effect on the cavity flow by the approximation to the flow past an ellipsoid. Not only the exact solution for the flow past the ellipsoid (Lamb, 1945) but also the linear solution (Weber, 1957) has been obtained. For a foil of small aspect ratio, Weber obtained constant velocity distribution on the elliptic foil by the application of slender body theory. In Figure 6 she compared the velocity increments at the center of the ellipsoids by four methods: the exact theory, the slender body theory, the linearized slender body theory, and the ordinary linear theory respectively. She also suggested the better approximation by the application of a factor to the velocity on the ellipsoid obtained by the linear theory. We use the right handed xyz-rectangular coordinate where x is in the direction of the uniform stream and z vertically upward. We consider an ellipsoid whose three axes are in the directions of xyz axes respectively. Then

the factor Weber suggested is written as

$$\frac{1}{\left\{1 + (\partial z/\partial x)^2\right\}^{\frac{1}{2}}}$$

This factor reduces the approximate velocity on the elliptical cylinder to the exact one in the two dimensional case. In the present paper this factor is applied to the approximate velocity at the center of the ellipsoid, i.e.

$$U = U_{max} \left\{1 + (\partial z/\partial x)^2\right\}^{-\frac{1}{2}}$$

If we approximate the cavity shape to this ellipsoid in the uniform flow, the drag due to the cavity can be obtained by the integration of the x component of the thrust over the front half surface of the ellipsoid. From Bernoulli's equation

$$C_p \equiv \frac{p - P}{\frac{1}{2}\rho U_o^2} = 1 - \frac{U^2}{U_o^2}$$

where U_o and P are the velocity and pressure at infinity respectively, and p is the local pressure on the surface of the ellipsoid.

Let the angle between the tangent plane to the ellipsoid and the x axis be denoted by α. Then

$$\frac{C_D}{A} = \int_{S_1} C_p \sin\alpha \frac{ds_1}{Ar} = \int_{S_2} \left(1 - \frac{U_{max}^2}{U_o^2 \left\{1 + (\partial z/\partial x)^2\right\}}\right) \frac{ds_2}{Ar}$$

where Ar is a given area, s_1 is the half front surface of the ellipsoid, and s_2 is the projection of the ellipsoid on the vertical center plane.

Since the ellipsoid can be represented as

$$z\,(x,y) = \frac{t}{2}\left\{1 - (1 - 2x)^2 - (y/s)^2\right\}^{\frac{1}{2}}$$

where t is the maximum thickness of the ellipsoid, s is the half span, and length ℓ is considered to be 1.

$$\frac{1}{1 + (\partial z/\partial x)^2} = \frac{4\,z^2/t^2}{t^2 + 4\,(1-t^2)\,z^2/t^2 - t^2\,(y/s)^2}$$

The integration of this expression on the projection of ellipsoid on the plane x = 0.5 is

$$\int_0^s \int_0^{\frac{t}{2}\{1-(y/s)^2\}^{\frac{1}{2}}} \frac{1}{1+(\partial z/\partial x)^2}\,dz\,dy = \left\{\frac{t}{1-t^2} - \frac{t^2}{(1-t^2)^{3/2}}\tan^{-1}\left(\frac{\sqrt{1-t^2}}{4}\right)\right\}\frac{s\pi}{8}$$

Hence if we represent the cavitation number

$$\sigma = \frac{P - p_{min}}{\frac{1}{2}\rho U_o^2} = \frac{U_{max}^2}{U_o^2} - 1$$

or

$$\frac{U_{max}^2}{U_o^2} = 1 + \sigma$$

we obtain

$$\frac{C_D}{Ar} = \left\{ \frac{(1+\sigma)\, t}{(1-t^2)^{3/2}} \tan^{-1} \left(\frac{\sqrt{1-t^2}}{t} \right) - \frac{t^2 + \sigma}{1 - t^2} \right\}$$

taking Ar as the maximum cross sectional area $Ar = \frac{ts\pi}{2} \ell^2$ in the dimensional quantity.

This shows that the drag coefficient does not include the semi-span s explicitly as long as we nondimensionalize it by the maximum cross sectional area and express C_D in terms of t and σ, but σ is a function of s and t. If we consider σ as an independent variable, t can be represented as a function of σ and s.

To obtain the free surface effect on the three dimensional cavity, we may approximate the three dimensional cavity for mathematical simplicity as like a rectangular wing of elliptic section. As far as the linear theory is concerned, the difference in the maximum velocities on the ellipsoid and on the rectangular wing of elliptic section is very small (see Weber, 1957). Due to Weber (1957), the increment of velocity due to the rectangular elliptic wing in the uniform flow can be approximated by the velocity produced by the source distribution

$$q(x') = 2U_o t \frac{1 - 2x'}{\left\{ 1 - (1-2x')^2 \right\}^{\frac{1}{2}}} \qquad \begin{array}{l} \text{in } -s < y < s \\ 0 < x < 1 \\ z = 0 \end{array}$$

i.e. the x component of the increment of the velocity at (x,y,z),

$$\frac{v_x(x,y,z)}{U_o} = \frac{1}{4\pi U_o} \int_0^1 \int_{-s}^{s} q(x') \frac{x - x'}{\left\{(x-x')^2+(y-y')^2+z^2\right\}^{3/2}} dx'dy'$$

Hence

$$\frac{v_x(0.5,0,0)}{U_o} = \frac{4}{\pi} ts \int_0^1 \frac{dx'}{\left\{1-(1-2x')^2\right\}^{\frac{1}{2}} \left\{(1-2x')^2+4s^2\right\}^{\frac{1}{2}}}$$

$$= \frac{4}{\pi} \frac{ts}{(1+4s^2)^{\frac{1}{2}}} K(k^2)$$

where $K(k^2)$ is the complete elliptic integral of the first kind with

$$k^2 = \frac{1}{1+4s^2}$$

As in the two dimensional case, the image source distribution for each x above the free surface is of the same magnitude but of the opposite sign to that of the real source distribution of the wing under the free surface. Hence the increment of the velocity due to the image also changes sign, i.e.

$$\frac{v_x(0.5,0,2d)}{U_o} = -\frac{4ts}{\pi}\int_0^1 \frac{(1-2x')^2\,dx'}{\left\{16d^2+(1-2x')^2\right\}\left\{1-(1-2x')^2\right\}^{\frac{1}{2}}\left\{(1-2x')^2+16d^2+4s^2\right\}^{\frac{1}{2}}}$$

$$= -\frac{4ts}{\pi}\int_0^1 \frac{dx'}{\left\{1-(1-2x')^2\right\}^{\frac{1}{2}}\left\{(1-2x')^2+16d^2+4s^2\right\}^{\frac{1}{2}}}$$

$$+\frac{4ts}{\pi}\,16d^2\int_0^1 \frac{dx'}{\left\{16d^2+(1-2x')^2\right\}\left\{1-(1-2x')^2\right\}^{\frac{1}{2}}\left\{(1-2x')^2+16d^2+4s^2\right\}^{\frac{1}{2}}}$$

putting $1 - 2x' = \cos\theta$

$$= -\frac{4tsk'}{\pi}\int_0^{\pi/2} \frac{d\theta}{(1+k'^2\sin^2\theta)^{\frac{1}{2}}} - \frac{64tsd^2\lambda k'}{\pi}\int_0^{\pi/2} \frac{d\theta}{(1+\lambda\sin^2\theta)(1+k'^2\sin^2\theta)^{\frac{1}{2}}}$$

$$= -\frac{4tsk'}{\pi}\,K(k'^2) - \frac{64}{\pi}\,tsd^2\lambda k'\,\Pi(\lambda,k'^2)$$

with

$$k' = \frac{1}{(1+16d^2+4s^2)^{\frac{1}{2}}} \quad \text{and} \quad \lambda = -\frac{1}{1+16d^2}$$

Hence the total increment of the velocity at $x = 0.5$, $y = 0$, $z = 0$ is

$$\frac{v_x(0.5,0,0)}{U_o} = \frac{4ts}{\pi}\left\{k\,K(k^2) - k'\,K(k'^2) - 16d^2\lambda k'\,\Pi(\lambda,k'^2)\right\}$$

If we use the linear relation

$$\sigma = \frac{2v_x(0.5,0,0)}{U_o}$$

we obtain

$$\frac{t}{\sigma} = \frac{\pi}{8s\left\{kK(k^2)-k'K(k'^2)-16d^2\lambda k'\Pi(\lambda,k'^2)\right\}}$$

This is computed by using the tables of Herbert Bristol Dwight (1958) and Heuman (1941). Figure 4 shows the maximum cavity thickness versus depth for each span. As in the two dimensional case, the maximum cavity thickness, $t/(\sigma\ell)$ at $d/\ell = 1$ is almost the same as that at $d/\ell = \infty$ for each span. Figure 5 shows the maximum thickness versus the span for each depth. The maximum cavity thickness $t/(\sigma\ell)$ at $s/\ell = 1$ is almost the same as that at $s/\ell = \infty$, or as in the two dimensional case for each depth.

REFERENCES

Auslaender, Jakob, "The Linearized Theory for Supercavitating Hydrofoils Operating at High Speeds Near a Free Surface", HYDRONAUTICS, Incorporated Technical Report 001-5, 1961.

Cheng, H. K., and Rott, N., "Generalization of the Inversion Formula of Thin Airfoil Theory", J. of Rational Mechanics and Analysis, Vol. 3, No. 3, May 1954.

Dwight, Herbert B., "Mathematical Tables of Elementary and Some Higher Mathematical Functions", 2nd Ed., Dover Publications, Inc., New York, 1958.

Fabula, Andrew G., "Application of 'Thin Airfoil' Theory to Slender Hydrofoils with Cut-Off, Ventilated Trailing Edge", U. S. Naval Ordnance Test Station, Pasadena Annex, Tech. Note P508-12, July 1960.

Fabula, Andrew G., "A Simple Approximation for Wall Effects on Cavity Size for Symmetrical Flows", U. S. Naval Ordnance Test Station, Tech. Note P508-14, October 1960.

Heuman, Carl, "Tables of Complete Elliptic Integrals", Journal of Math. and Physics, Vol. XX, pp. 127-206, 1941.

Johnson, V. E., Jr., "The Influence of Depth of Submersion, Aspect Ratio, and Thickness on Supercavitating Hydrofoils Operating at Zero Cavitation Number", Second Symposium on Naval Hydrodynamics, 1958.

Jones, Robert T., and Doris Cohen, "High Speed Wing Theory", Princeton University Press, 1960.

Morse, Philip M., and Feshbach, Herman, "Method of the Theoretical Physics, Part I", McGraw-Hill Book Co., 1953.

Muskhelishvili, N. I., "Singular Integral Equations", 2nd Ed., Moscow, 1946; Translated by J. R. M. Radok.

Perry, Byrne, "Evaluation of the Integrals Occurring in the Cavity Theory of Plesset and Shaffer", California Institute of Technology, Pasadena, Calif., December 1952, CIT Hydrodynamic Laboratory Report 21-24.

Plesset, M. S., and Shaffer, P. A., Jr., "Cavity Drag in Two and Three Dimensions", J. Appl. Phys., Vol. 19, No. 10, pp. 938, 1948.

Privalov, I. I., "The Cauchy Integral", Saratov, 1919. (Publ. separately by the Saratov Univ., 1918.)

Tulin, M. P., "Steady Two-Dimensional Cavity Flow about Slender Bodies", DTMB Report No. 834, 1953.

Weber, J., "The Calculation of the Pressure Distribution on Thick Wings of Small Aspect Ratio at Zero Lift in Subsonic Flow", Aeronautical Research Council Reports and Memoranda No. 2993, London, 1957.

Wolfgang Gröbner and Nikolaus Hofreiter, "Integraltafel Wien und Innsbruck", Springer-Verlag, 1958.

Wu, T. Y., "A Simple Method for Calculating the Drag in the Linear Theory of Cavity Flows", California Institute of Technology Report No. 85-5, August 1957.

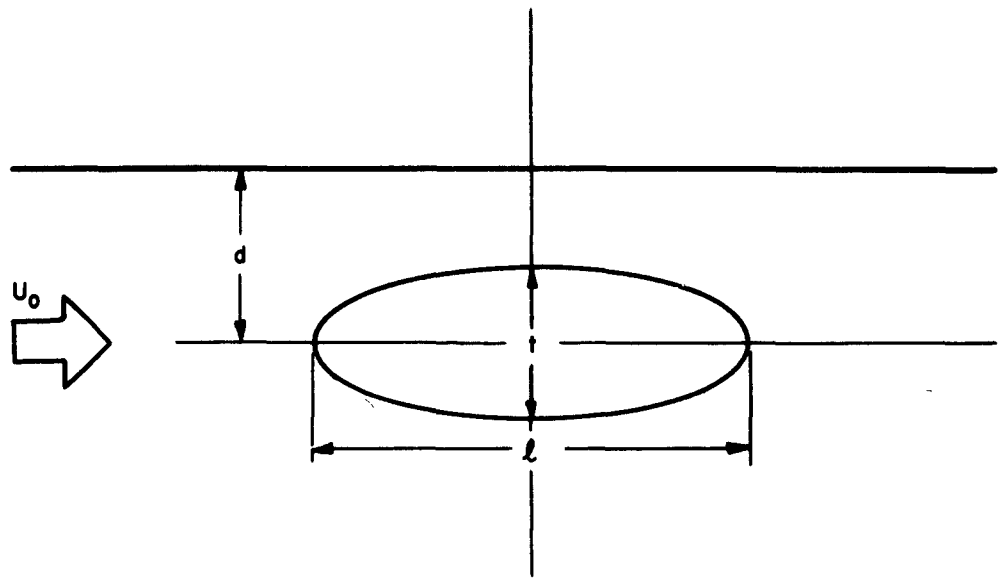

FIGURE Ia – SIMPLE CAVITY FLOW

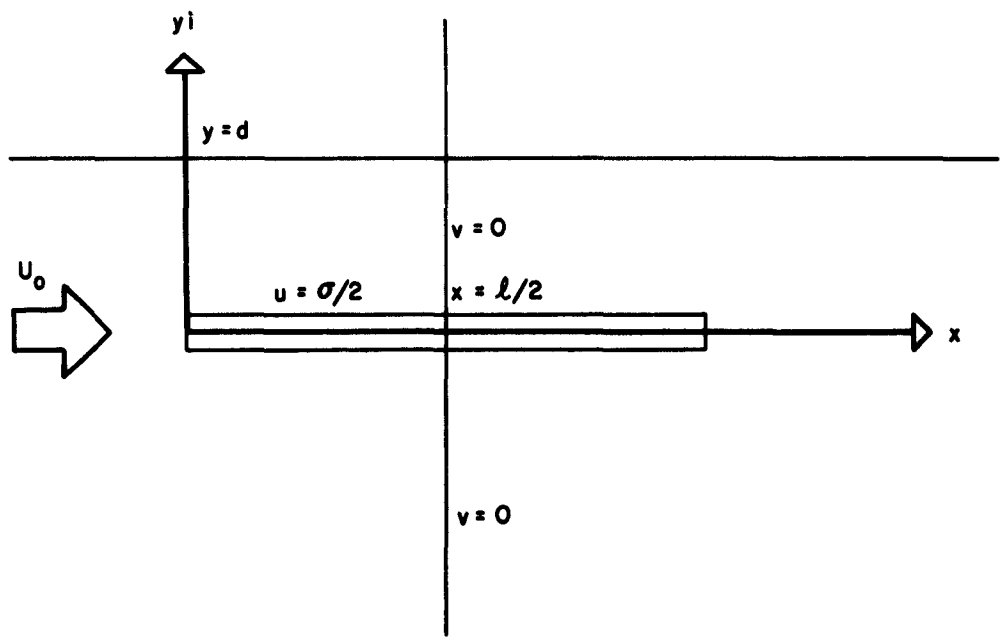

FIGURE Ib – LINEARIZED BOUNDARY CONDITIONS

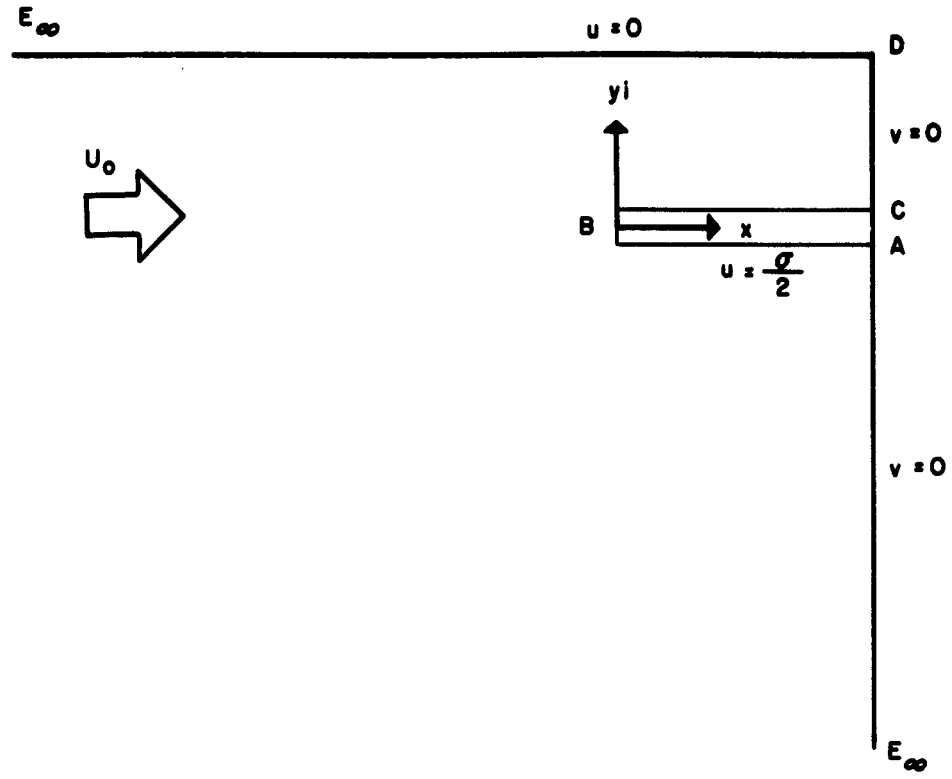

FIGURE Ic– Z PLANE

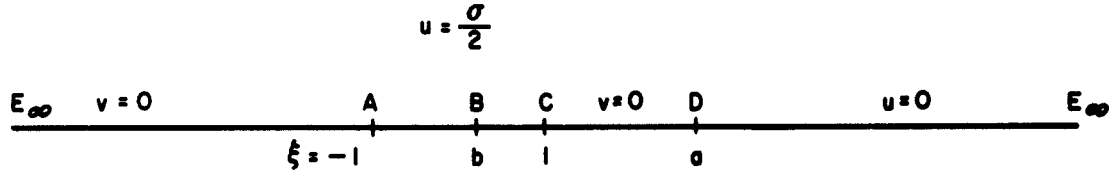

FIGURE Id– ζ PLANE

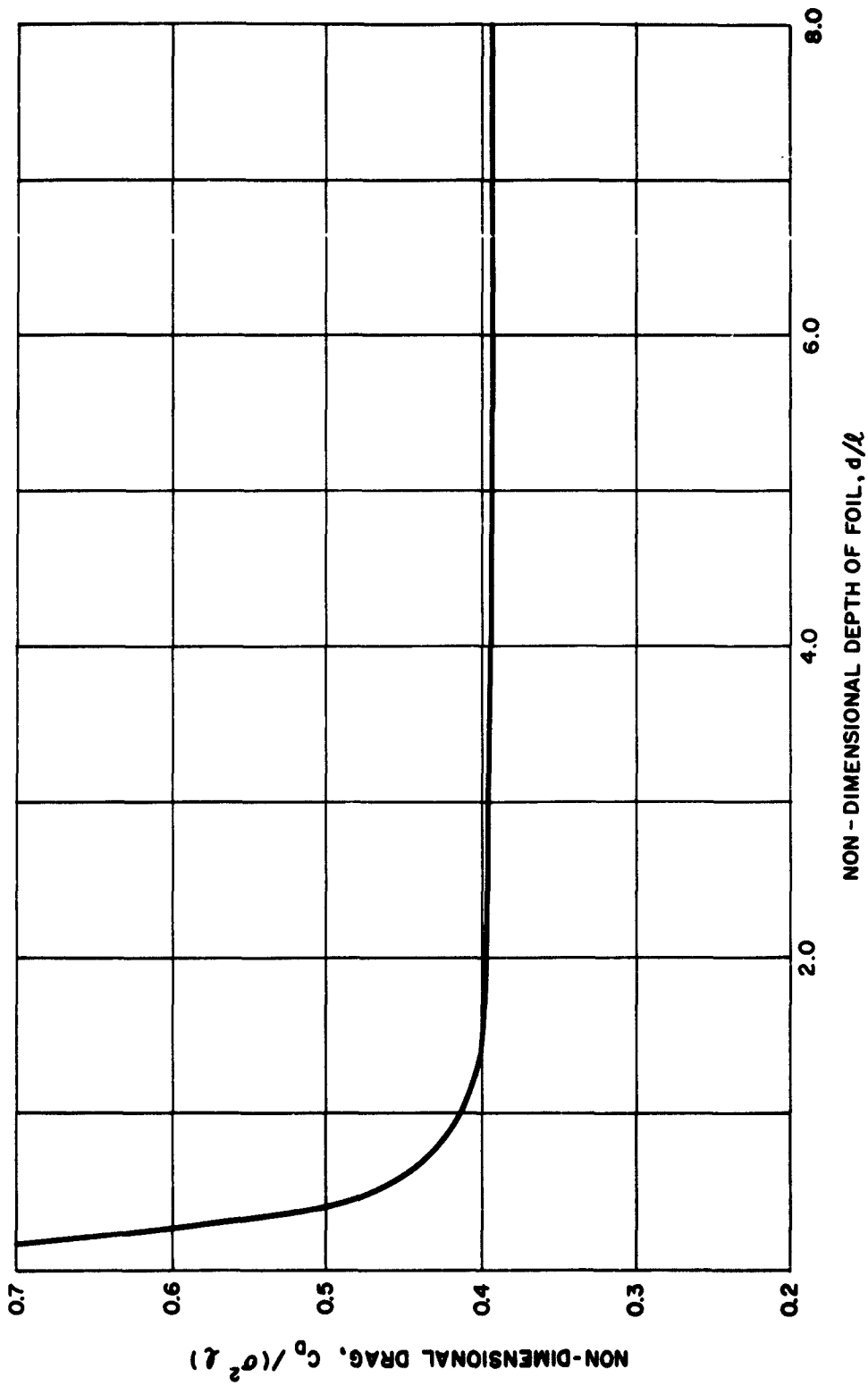

FIGURE 2- DRAG DUE TO A TWO-DIMENSIONAL CAVITY UNDER FREE SURFACE

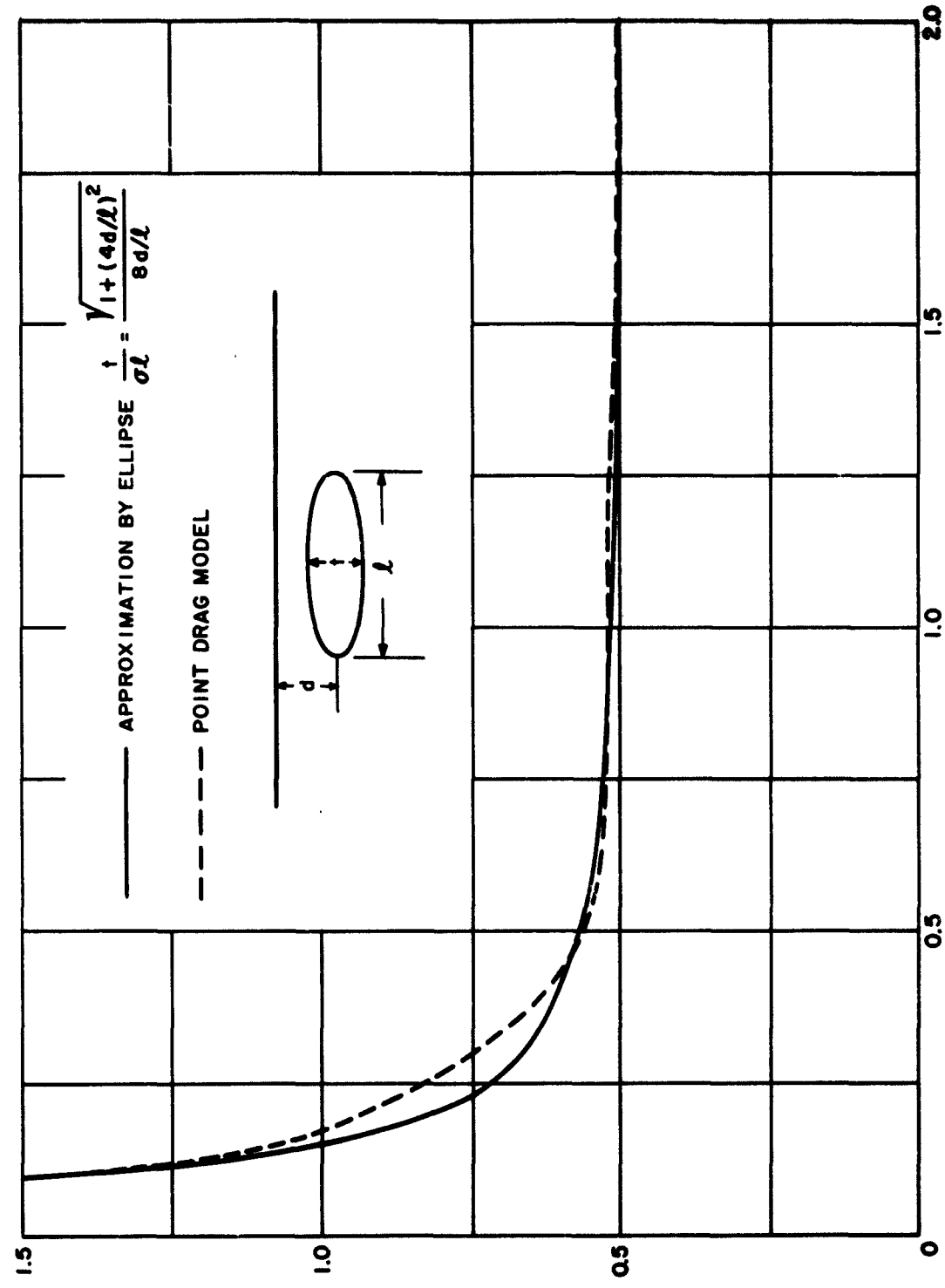

FIGURE 3 – MAXIMUM THICKNESS OF TWO-DIMENSIONAL CAVITY UNDER FREE SURFACE

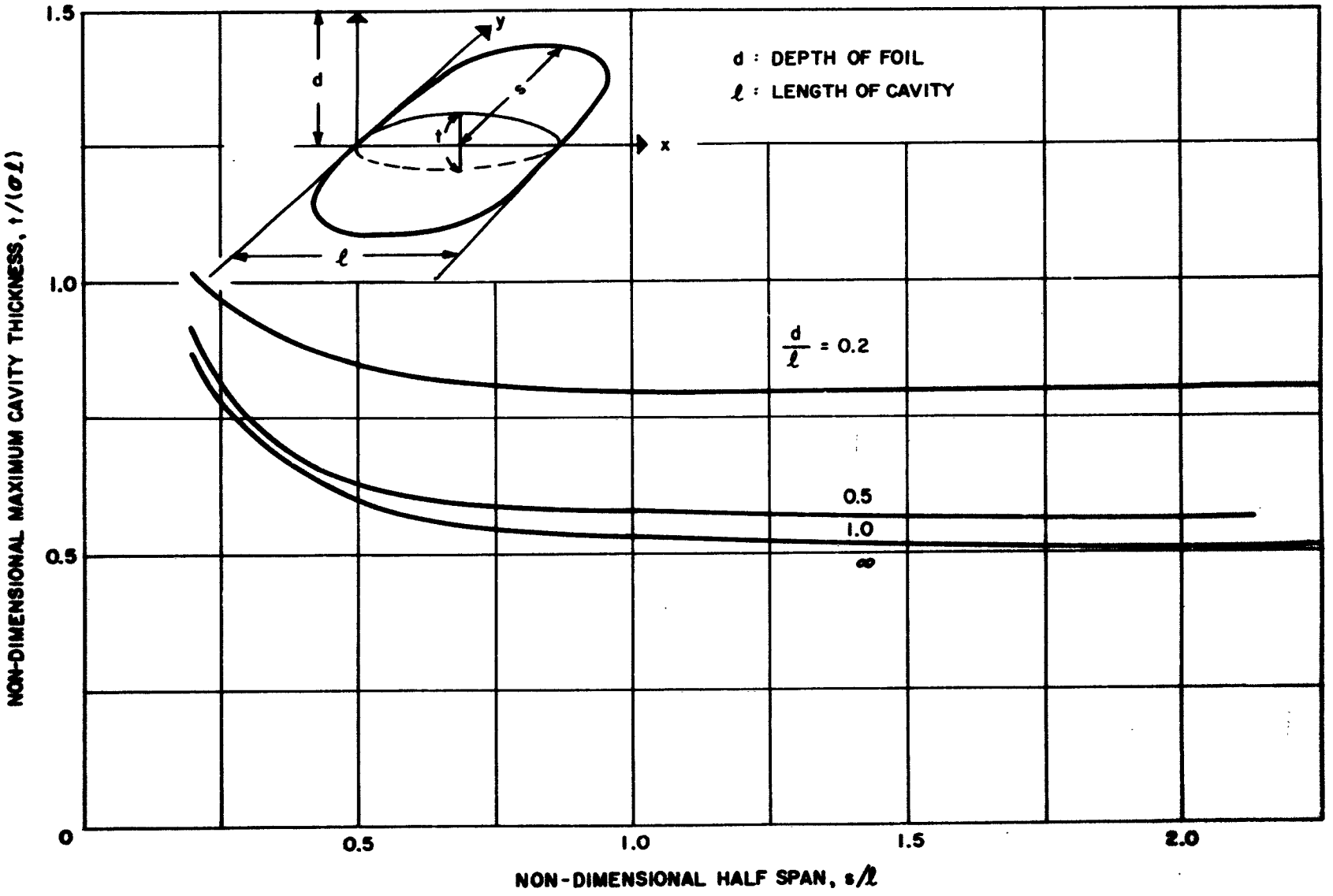

FIGURE 4- MAXIMUM THICKNESS OF THREE-DIMENSIONAL CAVITY UNDER FREE SURFACE

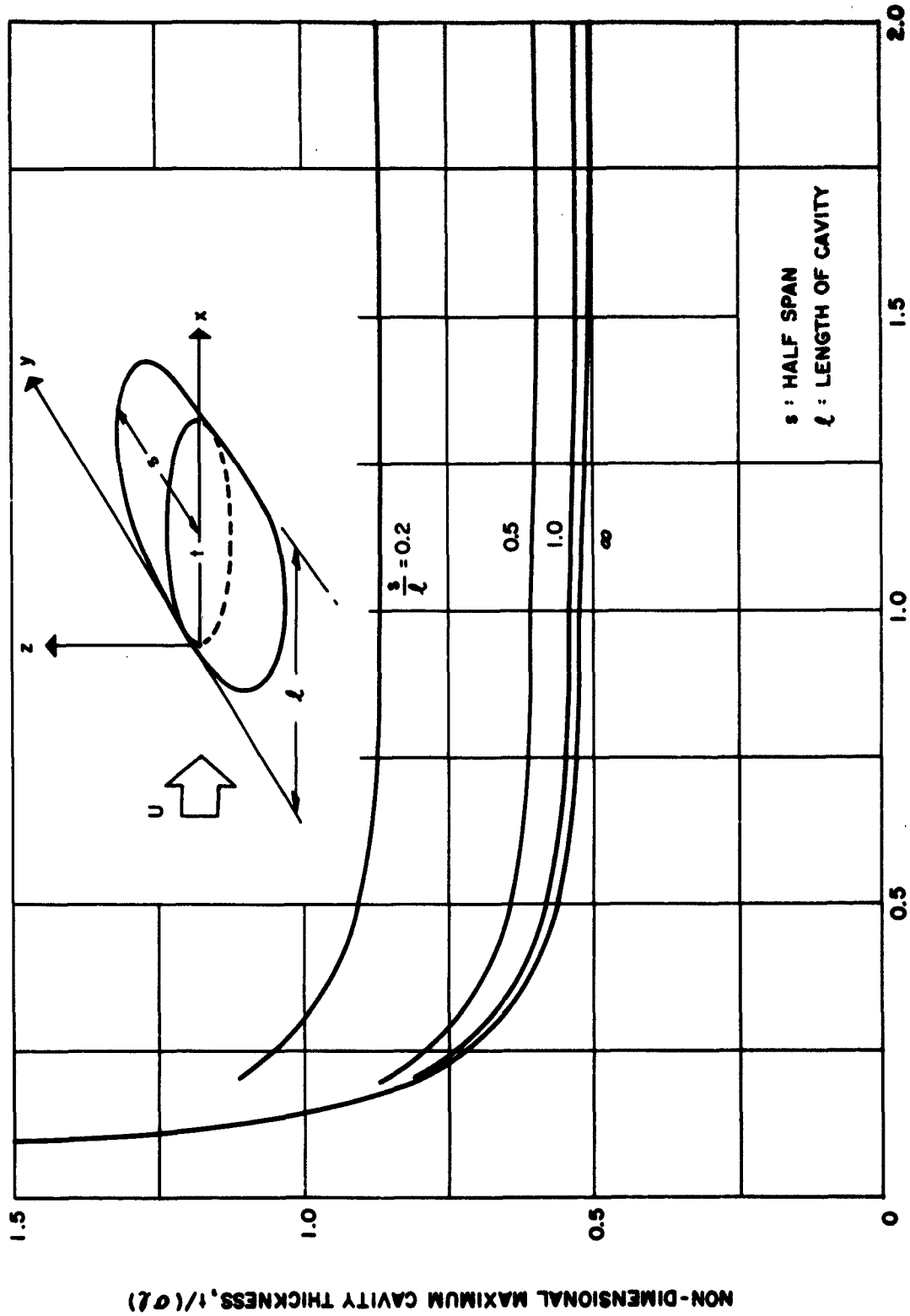

FIGURE 5- MAXIMUM THICKNESS OF THREE-DIMENSIONAL CAVITY UNDER FREE SURFACE

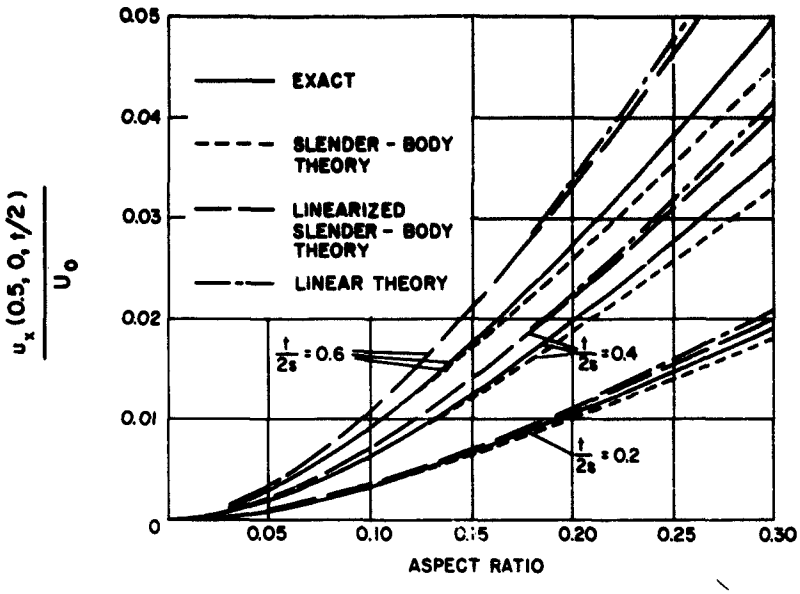

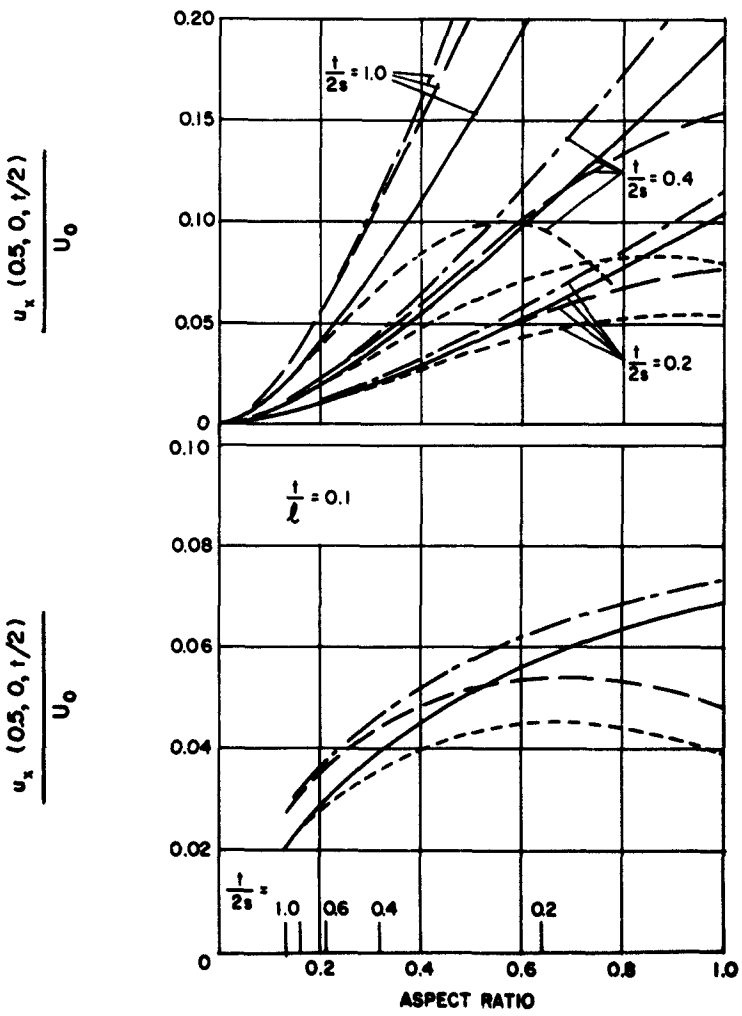

FIGURE 6- VELOCITY INCREMENTS ON ELLIPSOIDS

DISTRIBUTION LIST

BuShips Contract NObs-84296

	Number of Copies
Chief, Bureau of Ships (60) Navy Department Washington 25, D. C.	
ATTN: Code 106	1
Code 335	3
Code 410	1
Code 420	53
Code 442	1
Code 449	1
Chief, Office of Naval Research (2) Navy Department Washington 25, D. C.	
ATTN: Code 438	2
Commanding Officer and Director (6) David Taylor Model Basin Carderock, Maryland	
ATTN: Code 500	1
Code 513	1
Code 520	1
Code 526	1
Code 530	1
Code 580	1
Chief, Bureau of Naval Weapons (2) Navy Department Washington 25, D. C.	
ATTN: Code RAAD-343	1
Code R-52	1
Commander Armed Services Technical Information Agency Arlington Hall Station Arlington 12, Virginia	
ATTN: TIPDR	5

DISTRIBUTION LIST

Mr. John B. Parkinson Langley Aeronautical Laboratory National Aeronautics and Space Administration Langley Field, Virginia	1
Boeing Airplane Company Aero-Space Division Box 3707 Seattle 24, Washington	1
California Institute of Technology Pasadena, California ATTN: Professor T. Y. Wu Hydrodynamics Laboratory	1
Convair Hydrodynamic Laboratory Convair Division General Dynamics Corporation San Diego, California	1
Director, Stevens Institute of Technology Davidson Laboratory Castle Point Station Hoboken, New Jersey	1
Grumman Aircraft Engineering Corporation Marine Engineering Section Bethpage, Long Island, New York	1
Hughes Aircraft Company Systems Development Laboratories Culver City, California ATTN: Mr. W. N. Turner	1
Hydronautics, Incorporated 200 Monroe Street Rockville, Maryland	1
The Martin Company Baltimore 3, Maryland ATTN: Mr. John D. Pierson	1

DISTRIBUTION LIST

Massachusetts Institute of Technology Department of Naval Architecture and Marine Engineering Cambridge 39, Massachusetts	1
Director University of Minnesota St. Anthony Falls Hydraulic Laboratory Hennepin Island Minneapolis 14, Minnesota	1
Southwest Research Institute Department of Applied Mechanics 8500 Culebra Road San Antonio 6, Texas	1
Technical Research Group, Inc. 2 Aerial Way Syosset, New York	1
Chief of Naval Operations Navy Department Washington 25, D. C. ATTN: Capt. N. H. Fisher, OP-712	1